Journal of Building Pathology and Rehabilitation (2022) 7:38
https://doi.org/10.1007/s41024-022-00176-z

RESEARCH ARTICLE

Reduction of concrete permeability using admixtures or surface treatments

Vanessa Giaretton Cappellesso[1] · Natália dos Santos Petry[2] · Márlon Augusto Longhi[2] · Angela Borges Masuero[2] · Denise Carpena Coitinho Dal Molin[2]

Received: 28 October 2021 / Revised: 28 February 2022 / Accepted: 2 March 2022 / Published online: 27 March 2022

Abstract

The durability assurance in reinforced concrete is necessary during the design conception and mix design as a preventive measure. Permeability in cementitious materials is a crucial durability indicator that can be influenced by many factors, from capillary porosity to cracks. Under those circumstances, it might be helpful to have concrete with the ability to reduce permeability. In this paper, the effectiveness of incorporating a crystalline admixture, both as an admixture and surface treatment, through characterisation tests, durability tests, and self-healing analyses. A concrete with silica fume as an admixture was also produced for comparison to the use of crystalline admixture (CA). The silica fume showed more efficiency in all assessed properties relative to both the reference and CA for condition with limited water availability. Crystalline admixture is also beneficial over reference concrete when used as an admixture, increasing the compressive strength and decreasing the ingress of chloride and carbon dioxide. The concrete with surface treatment had similar behaviour of reference concrete. Additionally, healing products from the use of crystalline admixture take the form of a needle shape in concrete.

Keywords Concrete · Permeability · Durability · Crystalline admixture · Silica fume

1 Introduction

Several factors influence concrete durability, where physical and chemical effects assist in the deterioration of the structure [1–4]. This process can be associated with intrinsic materials properties and exposure conditions [3, 5], and external factors such as incomplete consolidation and inadequate curing process [6]. Using different materials to protect and prevent the ingress of the aggressive substances from the environment might reduce deterioration [1, 4, 7–9]. These preventive actions influence the preservation of natural resources and contribute to sustainability [5, 10–12] by improving the service life [1, 5, 11, 13–15].

One of the most effective ways to mitigate concrete deterioration is decreasing its permeability to limit fluid transport mechanisms. Permeability is associated with the amount of the voids, capillaries and/or cracking, which are considered the gateway to aggressive agents [1, 6, 16, 17]. In the case of cementitious materials, the deterioration rate increases in more permeable materials [2, 6, 18]. Some ways to improve durability associated with permeability reduction are through matrix densification, self-healing or surface treatment as a physical barrier to the penetration of water,

✉ Vanessa Giaretton Cappellesso
vanessa.cappellesso@ugent.be

Natália dos Santos Petry
nataliapetry@yahoo.com.br

Márlon Augusto Longhi
marlonlonghi@gmail.com

Angela Borges Masuero
angela.masuero@ufrgs.br

Denise Carpena Coitinho Dal Molin
dmolin@ufrgs.br

[1] Magnel-Vandepitte Laboratory for Structural Engineering and Building Material, Department of Structural Engineering and Building Materials, Ghent University, Technologiepark Zwijnaarde 60, 9052 Ghent, Belgium

[2] Laboratório de Materiais e Tecnologia do Ambiente Construído (LAMTAC), Núcleo Orientado Para Inovação Na Edificação (NORIE), Universidade Federal do Rio Grande do Sul, Osvaldo Aranha Avenue, 99, Porto Alegre, Brazil

ions and gases [1, 12, 13, 19]. Several studies have been conducted to produce and test new products to decrease permeability as a preventative method [7, 11, 13, 14, 20, 21] or stop fluid movement in finished structures for repair [1, 12, 18], which can both contribute to the extension of service life [11].

Some of these products, such as crystalline admixture [5, 9, 10, 14, 15, 22–29], have their chemical compositions kept undisclosed by the companies that produce them for to intellectual property protection. This makes complete scientific understanding difficult, and results can vary between manufacturers [30]. Crystalline admixtures (CA) have strength recovery and crack sealing properties [10, 11, 14, 28, 29]. The product reacts with moisture in fresh concrete and with cement hydration products [14], resulting in an insoluble crystalline structure in concrete pores and capillaries, which reduces capillary porosity and permeability [24], and allows crack healing [14]. Crack closure described in several studies is related to the autogenous healing process, but with greater intensity and without dispensing with the need for water [10, 11, 14, 21]. Most product specifications for crystalline admixtures have the capacity to seal cracks up to 0.4 mm.

The ACI TC 212 report [6] states that the concrete compounds reacting with CA are tricalcium silicates. Other authors [21, 31] indicate that the calcium hydroxide ($Ca(OH)_2$) formed during cement hydration transforms into calcium carbonate ($CaCO_3$), even in a submerged environment [10], and can form stable carbonate crystals. The higher pH of these products favours the calcium carbonate precipitation due to the higher concentration of Ca^{2+} close to the surface, contributing to healing [21].

Some practical applications were conducted with a crystalline admixture product [32] and verified with visual analyses. A reduction in water leakage was noticed over time. The behaviour of these products is still partially unknown, but the expected results guarantee employment based on the improved properties that they obtain. There are many variations in literature regarding the levels that are used for CA, from 0.5% [17], 0.8% [14], 1.0% [10, 14], 1.5% [17, 21], 2.0% [33], to 4.0%.

Another way to reduce permeability is incorporating pozzolanic cement and/or supplementary cementitious material (SCMs) into the concrete mix design, which is widely implemented in literature [2, 34–43]. SCMs are commonly used in concrete since they improve the microstructure and durability of concrete [35, 42–53]. The use of admixtures from commercial or mineral origins is one alternative that can contribute to the use of waste material as SCMs. It can improve the physical–mechanical properties and contribute to the autogenous self-healing capacity of the cementitious matrix. Hence, the repair costs and maintenance of concrete structures could be reduced due to the improvement of these properties.

Given the importance of producing less permeable and more durable concrete structures, this paper aims to analyse the performance of using a crystalline admixture as a surface treatment and as an admixture, and another concrete with silica fume, for comparison purposes, concerning permeability properties and self-healing. This study provides new insights into the effectiveness of a crystalline admixture in reducing permeability and improving durability. The knowledge obtained will give further information about the materials, reactions and self-healing, and will be essential to design concrete with a higher durability.

2 Materials

2.1 Cement

A commercial pozzolanic cement was used (Brazilian cement type CPIV) of strength class 32, equivalent to type IP, according to ASTM C 595 [54]. Following the Brazilian standard ABNT 16,697 [55], this cement type requires the use of 45 to 85% of clinker and calcium sulphate. It allows the use of 15 to 50% of pozzolanic materials; for this study fly ash was used.

The specific area of this cement is 4900 cm^2/g. The bulk specific gravity is 2.59 g/cm^3. The setting times had a start at 5 h 55 min and end at 8 h 15 min, according to Brazilian standard, NBR 16,607 (ABNT 2018a). The compressive strength met the regulatory limits of the NBR 7215 [57], with values of 17.7 MPa at three days (required $\geq$ 10.0), 22.8 MPa at seven days ($\geq$ 20.0), and 36.2 MPa at 28 days ($\geq$ 32.0). This type of cement was used due to a large amount of fly ash in its composition. The replacement of clinker by the mineral admixture can contribute to cementitious matrix's mechanical properties and durability [58, 59]. It can also induce a higher formation of product to allow self-healing to occur [60, 61].

2.2 Aggregates

The fine and coarse aggregates were characterised for sieve analysis according to NBR NM 248 (ABNT 2003). The fine aggregate is quartz-based sand with a particle fineness modulus of 2.28. The bulk specific gravity of sand culminated in 2.58 g/cm^3 (ABNT 2009). The coarse aggregate used is basaltic-based gravel in two different particle sizes. The first one has 12.5 mm as maximum size, the bulk specific gravity of dry aggregate about 2.95 and water absorption of 1.43% (ABNT 2017). The last has 25 mm as a maximum size, the bulk specific gravity of dry aggregate about 2.91 and water absorption of 0.66%. Figure 1 presents the particle-size distribution of the aggregates.

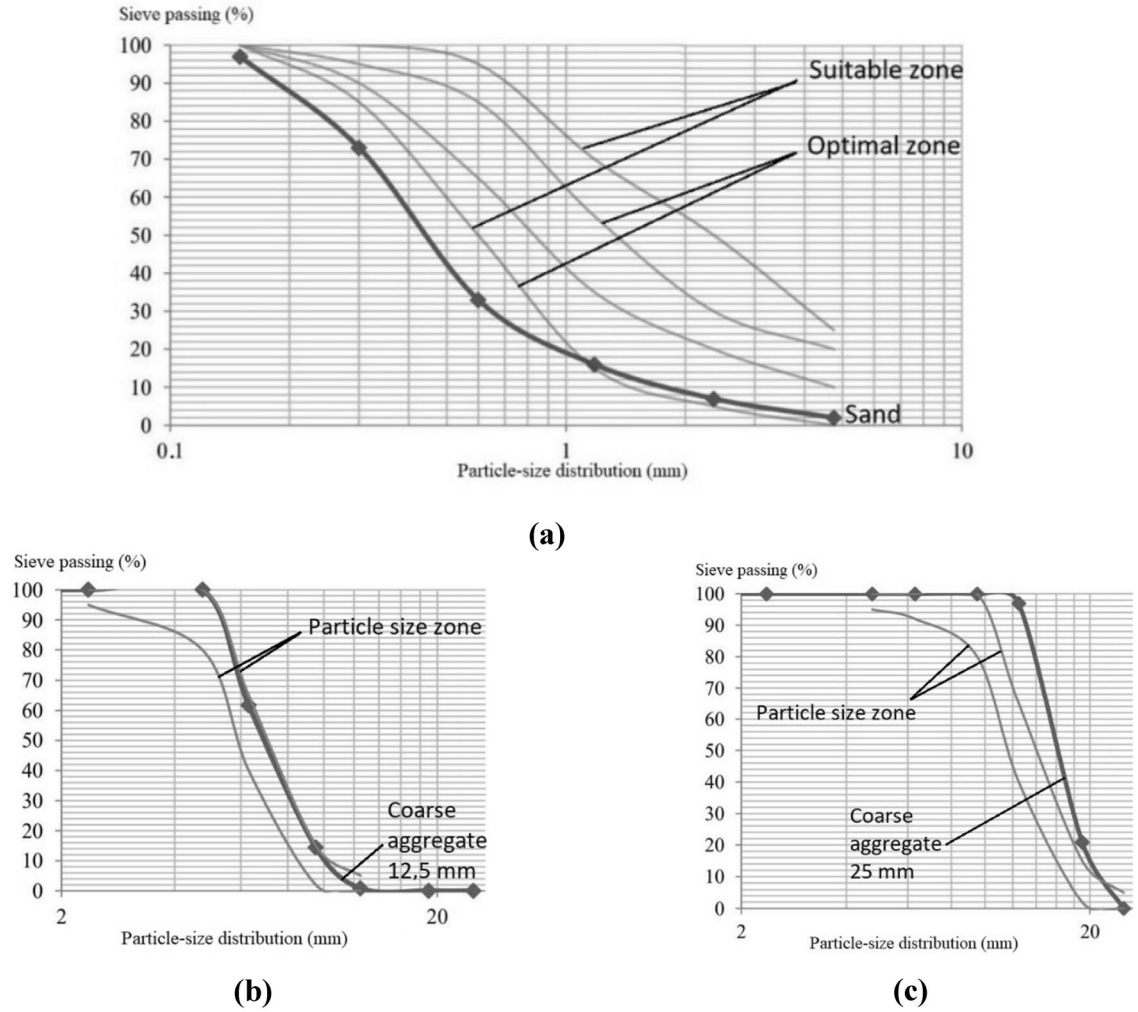

Fig. 1 Particle-size distribution of the **a** fine aggregate, and coarse aggregate with maximum size **b** 12,5 mm and **c** 25 mm

2.3 Chemical admixtures

Two chemical admixtures in the mix design were used. A polyfunctional water reducing plasticiser admixture with density 1.160 ± 0.02 g/cm^3, and a chemical-based polycarboxylate superplasticiser with a density of 1.095 ± 0.02 g/cm^3 and $40.0 \pm 2\%$ solids, and classified as Type A and F according to ASTM C 494 (ASTM).

2.4 Crystalline admixture

The crystalline admixtures were used as an admixture and as a surface treatment. These products are a particular type of permeability reducer admixtures (PRAs), as reported by the ACI Committee 212 [6]. In contrast with other coatings that are water-repellent or hydrophobic, these materials are hydrophilic [6]. They are water friendly, react efficiently and perform well [8, 9, 11, 24].

The crystalline waterproofing/admixture used as an admixture is composed of Portland cement (40–70%), quartz sand (5–10%) and active chemicals (10 to 30%), according to the manufacturer's description and other researches [10, 14]. This product has a grey powder appearance, without odour and pH solution between 10 to 13, and a density of 2.920 g/cm^3. The XRF test was also performed to characterise the material; the oxide composition is shown in Table 1. A Panalytical Epsilon equipment was used for semi-quantitative analysis using an Omnian package. The study was performed using a silver

Table 1 Oxides composition of crystalline admixture

Oxide	CaO	SiO_2	MgO	SO_3	Al_2O_3	Fe_2O_3	K_2O	TiO_2	SrO	Cl	MnO	ZnO	V_2O_5	Na_2O
(%)	60.61	13.07	4.81	4.43	3.80	2.81	1.22	0.24	0.14	0.11	0.07	0.05	0.02	0.00

(Ag) anode with SDD5 detector, 50 kV power, 100 µA current, Cu-500 copper filter and air atmosphere. In the XRD test the crystalline phases present were identified in this material, and it was found to contain C_3S (alite); C_2S (belite); C_3A (calcium aluminium oxide); C_4AF (iron aluminium calcium oxide); gypsum (calcium sulfate hydrate); portlandite (calcium hydroxide – $Ca(OH)_2$); periclase (magnesium oxide – MgO). The recommended dosage on the cement mass is between 0.8% to 1.0%. In this paper, the content used was 0.8%.

The crystalline admixture used as a surface treatment is composed of Portland cement (10–50%), quartz sand (10–40%) and active chemicals (30–60%), according to the manufacturer's description. This product has a grey powder appearance, with an odour like cement, pH solution between 10 to 13, and density of 1.450 g/cm^3. Surface treatment is intended to precipitate inside the pores, bonding with the substrate [1, 19] to reduce capillary porosity [66].

The manufacturer recommends mixing the product with water with the proportion of 5:2.5 (crystalline admixture: water) in mass. According to the operating instructions, it was applied on the concrete surface in two layers. The second layer must be applied before the first dries. The ideal condition of the specimen is to be saturated with a dry surface. After casting, the product should be consumed within 20 min. Subsequently, the surface treatment is applied, and the treated areas should be kept moist for five days.

Furthermore, the manufacturer indicates that the product develops the same performance whether the sample was smoothed or not. Therefore, specimens were tested with and without smoothing the layer. It was performed manually using sandpaper with a grit size of 80 µm.

This product is commonly used in structures with high water availability, such as reservoirs, water and effluent treatment plants, tunnels, foundations, and other structures that require a waterproofing system [14, 32]. However, in this study, conditions with lower humidity levels were tested.

2.5 Silica fume

Silica fume is also used and will be compared to crystalline admixture due to the expected similar behaviour. In general, silica fume increases durability due to the reduction in permeability and densifications of cementitious matrix [42, 44–50, 52, 53]. The activation mechanism is the same as the pozzolanic reaction because the silica reacts with the hydroxyls present on the pore surface, forming C–S–H [19]. However, part of this material remains unreacted in filler forms and becomes reactive in suitable exposure conditions. The use of silica fume can promote self-healing processes, but it is also essential to understand how it works and compare the performance to a crystalline admixture [19]. Some researchers have already employed silica fume to stimulate autogenous self-healing [49, 67].

The oxide composition of silica fume is shown in Table 2, where the XRF test conditions were the same used for the crystalline admixture. The bulk specific gravity of silica fume is 2.20 g/cm^3.

3 Experimental program

In this study, the efficiency of concrete using different admixtures as well as surface application forms are evaluated. Silica fume was used exclusively as admixture, and a crystalline powder was used in two different ways: as an admixture and surface treatment. In the case of surface treatment, one sample was smoothed and the other was untreated. Five different combinations in concrete were tested: reference concrete (REF), concrete with crystalline admixture surface treatment that was smoothed (STS) and not (STN), concrete with crystalline admixture (CA) and concrete with silica fume admixture (SF). The unit mix design of concrete is 1:1.50:2.34 (cement: fine aggregate: coarse aggregate in two different sizes), with a water/cement ratio of 0.41. To fix the w/c ratio and allow consistency between 200 ± 30 mm in all concretes, according to NBR NM 67 (ABNT 1998), two different types of admixture were used: one was a polyfunctional admixture (0.60% of cement mass), and other a superplasticiser (0.24% of cement mass). The crystalline admixture was used in a proportion of 0.80% on the cement mass and silica fume, a ratio of 10% on the cement mass. After concrete casting, the samples were moulded, kept in the moulds for 24 h and then stored in a humidity chamber at 23 ± 2 °C and relative humidity (RH) higher than 95%, where they remained until testing. This experimental program was based on a previous paper [25].

3.1 Opening cracks

Crack opening was performed at 28 days of curing, as reported in previous papers [20] using a four-point bending test. A load of (0.45 ± 0.15) MPa/s was applied, the load stopped when the first crack appeared. After crack opening, all samples were evaluated using a crack gauge. Thus, only specimens with cracks smaller than 0.4 mm were used in the analysis, as recommended by the supplier of the crystalline admixture.

Table 2 Oxides composition of silica fume

Oxide	SiO_2	K_2O	CaO	MgO	Al_2O_3	SO_3	Fe_2O_3	P_2O_5	Na_2O	MnO
(%)	92.36	0.86	0.77	0.24	0.20	0.15	0.14	0.11	0.06	0.03

3.2 Exposure environment

The curing of the specimens for compressive strength, total absorption and under pressure water penetration tests was made in a humidity chamber (RH higher than 95% and temperature 23 ± 2 °C) during 28 days after casting. The specimens were moisture-cured for 30 days for the carbonation test, then stored for five days in a climate chamber (RH of 75 ± 5% and temperature of 20 ± 2 °C) until humidity constancy, then placed in a carbonation chamber (5% CO_2). In the chloride penetration test, the specimens were cured in a humidity chamber for 28 days, then three more days in a climate chamber, and then the test was performed.

In the self-healing analysis, the specimens were subjected to moisture-curing for 15 days. Then they were stored in a climate chamber for 28 days (crack opening day). Subsequently, surface treatments were performed on the specimens. This treatment requires five days of moisture-curing. Then, to maintain the curing standard, all samples, even those that did not receive surface treatment, were also kept in a moist environment in the same period. Afterwards, they were placed in a climate chamber, where they remained throughout the analysis. Apart from optical microscopy analysis, there was no change in the exposure environment after 140 days in a climate chamber. From this age, the samples were kept in a humidity chamber.

Researchers in this field report that water supply is essential for self-healing process, whether crystalline admixture or other supplementary cementitious materials are used [10, 14, 21, 24, 26]. Due to the hydrophilic characteristics, the crystalline admixture can capture moisture in the air and react with it [8, 10]. At an early age, cracked concrete performance with the CA is improved compared to a more mature concrete with higher air moisture [38]. Some researchers realised that this environmental condition did not demonstrate performance superior to the submerged condition [10, 11, 14, 16]. However, this research aimed to evaluate the product's performance in less favourable conditions, simulating real conditions of concrete exposure on-site, with considerable humidity (RH of 75 ± 5%), but without immersion in water.

3.3 Methods

3.3.1 Characterisation tests

The compressive strength test was performed in concretes after 28 days of curing, using a Universal testing machine EMIC, adopting the procedure recommended by NBR 5739 (ABNT 2018b) using cylindrical samples with dimensions of 100 × 200 mm. A load of (0.45 ± 0.15) MPa/s was applied until the specimen failed. Seven specimens were cast for each combination.

The total absorption test is the same as presented in a previous paper [25], recommended by the NBR 9778 (ABNT 2005) using the same size of samples from compressive strength and after 28 days of curing. This analysis allows determining the absorption, voids, density of the dried sample, density of the saturated sample and normal density. Four specimens were cast for each combination.

3.3.2 Durability tests

The test of under pressure water penetration was performed using the same methodology as a previously published paper [25]. Four specimens of each concrete type were tested, which were individually adhered to a PVC pipe with 100 mm diameter and 3 m long by use of a polyurethane mastic. Then, the PVC pipes were filled with water until the pre-set level, until a pressure on the upper face of the specimen 30 kPa was achieved. The pressure was kept constant during the test. After seven days, the pipes were emptied, and the specimens were split. Photographic records were made of the specimens' internal faces to quantify the dry and wet areas. Quantification was performed using AutoCAD software by manually selecting areas.

The carbonation test was performed by an accelerated process, and two specimens were analysed for each concrete with dimensions of 320 × 90 × 90mm^3. The specimens were stored in an accelerated carbonation chamber with a 5% CO_2 concentration with the top and bottom edges of the samples sealed with solid paraffin to waterproof them and allow carbonation only across lateral faces. This process was remade after each disruption to verify the carbonation depth at the ages of 78, 100, 120, 142, 162 and 176 days. Freshly fractured slices were sprayed with 1% phenolphthalein solution dissolved in ethyl alcohol. The remaining part of the specimen was stored back in the carbonation chamber, and the broken surface was waterproofed. AutoCAD software was used to scale the images to quantify the carbonation depth. On each lateral face, five measurements were recorded, totalling 20 depth measurements for each slice, disregarding the corners. The carbonation result is the average of the measurements taken.

The accelerated test method of ASTM C 1202 (ASTM 2019) was used to determine chloride penetration in concretes. Ten specimens were cast, two for each type of concrete tested. The specimens were cylindrical with dimensions of 95 × 190 mm. From each sample, two slices measuring 51 ± 3 mm in thickness were used, resulting in four pieces for each type of concrete, totalling 20 slices for the test. The slices that received the surface treatment had the product applied only on the faces where there was contact with the solutions used in the trial. ASTM C 1202 (ASTM 2019) provides a classification of concretes for chloride penetration resistance following the current intensity and the Coulombs

through the load. The samples were split in half to spray silver nitrate solution (0.10 N in deionised water) to verify the penetration depth of the chlorides. AutoCAD software was used to quantify chloride penetration areas.

3.3.3 Self-healing test

The ultrasonic wave propagation using ultrasonic wave transmission velocity was performed according to ASTM C 597 (ASTM 2016). The equipment used had Proceq Pundit Lab transducers of 28 mm diameter and a frequency of 150 kHz. An indirect transmission method at four different points was used, in which the transducers were placed on the lower side of the specimen. The crack location was marked in the centre of the sample and used as the reference point. This method has already used in others researches [10, 73–79].

The high resolution scanning electron microscopy (SEM) was performed using an FEI Quanta 650 FEG, in the Brazilian Nanotechnology National Laboratory (LNNano). The equipment was equipped with an Everhart Thomley SED (secondary electron detector) and an In-column detector (ICD) for secondary electrons in beam deceleration mode. It works with a high-resolution Schottky field emission (FEG) and accelerated voltage between 200 V and 30 kV in a probe current ≤ 200 nA. The samples used were superficial fragments of the specimens. The samples were dried at 60 °C for 2 h, placed in the carbon tab, and coated with gold for 60 s with a current of 40 A. This technique was used to identify the products formed in autogenous self-healing developed by the reference concrete, those developed using crystalline admixture and silica fume. This method is widely used in other papers [5, 10, 11, 14, 17, 21, 22, 35, 36, 78, 80–83].

4 Results

4.1 Characterisation tests

The concrete characterisation was performed by the compressive strength and total water absorption tests. Compressive strength is shown in Fig. 2a and water absorption and void index in Fig. 2b.

It is possible to observe in Fig. 2a that the use of crystalline admixture as surface treatment (STN) practically does not change the compressive strength when compared to the reference concrete (REF). This behaviour was expected since the influence of the product, in this case, is only superficial and does not change the hydrate products formation. When used as an admixture, the CA increased the strength by 13%, a similar value found by other research [9]. This cement composition allows the formation of different products, especially at early ages of hydration, so this behaviour may be associated with the appearance of ettringite as reported previously [29], where the increase in compressive strength was also observed in mature ages. Other researchers also registered increased strength with the use of a similar product [8–10, 17]. This effect may also be related to the filler effect, contributing to the filling of voids [9]. However, it may have worked as a cement hydration activator, improving the cement paste microstructure [84], as well as enhancing the reactions of the silicates present in the product with calcium hydroxide resulting in the formation of the C–S–H [11, 34]. The addition of silica fume (SF) proved to be the most efficient for this property, providing an increase of 27% in compressive strength compared to the reference concrete (REF). This behaviour is associated with the pozzolanic

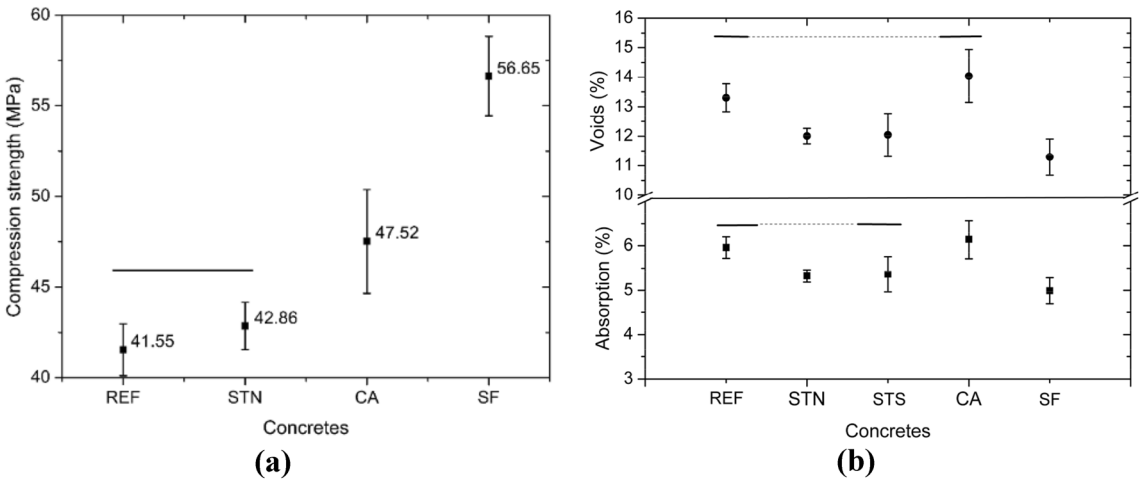

Fig. 2 Results of characterisation tests for the analysed concretes **a** compressive strength; **b** water absorption and voids. The horizontal bar above some combinations refers to the statistical analysis of variance and indicates no statistical difference between combinations identified with a continuous line

reaction where secondary C–S–H is formed due to the dissolution of silica fume in contact with portlandite. Silica fume also serves as a nucleation point to assist in the cement hydration process contributing to increase strength by matrix densification [2, 33, 58, 59, 85, 86] and also reducing permeability [2, 7, 43, 51, 58, 59, 86–88]. The reduction in permeability and densification can be seen in Fig. 2b due to the low water absorption and low voids found for SF concrete.

Different materials were considered mathematically significant by a cross-factor variance analysis using Statistic 7 software. Additionally, by Fisher's test, it was found that the reference concrete (REF) and the surface treated concrete (STN) are equivalent to each other.

In Fig. 2b, the voids index and water absorption behaviour are similar because the factors are directly proportional. It can be observed that the use of crystalline admixture as the surface treatment reduces the water absorption for both the smoothing (STS) and non-smoothing (STN) samples, as they also reduce the void index. The reduction was expected since the surface treatment with this product is intended to seal the concrete surface and prevent water ingress. Products with waterproofing characteristics that are considered a pore protection system have little influence on the voids of the cementitious matrix [89, 90]. This pore closure process is explained by Bertolini [90] that the late reaction of the cement releases the portlandite, which reacts with pozzolans and causes the clogging of pores.

CA concrete shows an increase in water absorption compared to the REF concrete, a fact not expected since there was an increase in strength. It can be explained by a possible variation in the size and quantity of capillary pores contributing to increased hygroscopicity of the material. In addition, the product has hydrophilic characteristics [6, 8, 9, 11, 24]. At first contact with water, the CA product tends to have hygroscopic characteristics until the capillary porosity is sealed. After this sealing, the product makes the matrix impermeable and prevents the fluids entrainment. This phenomenon can increase the amount of water absorbed. Previous studies showed that crystalline coating took 12 days from casting to perform efficiently [91]. As for strength, smaller and well-distributed pores may not influence the loss of matrix strength [31].

For water absorption factors and voids index, the use of the different materials was considered significant, which was performed by cross-factor variance analysis. By Fisher's Test, it was found for water absorption that only STS concrete does not differ significantly from REF concrete. Already STN concrete and concretes with additions of CA and SF are statistically different from the REF concrete. And for the void index, only CA concrete does not differ significantly from REF concrete.

Table 3 shows the densities of the dried samples, saturated samples, and real density. Densities were obtained by the total absorption test and without significant differences between them. Therefore, the concrete properties increase due to the interconnection among the pores instead of the distribution or size of the pores themselves.

Table 3 Concretes densities

Concretes	Average densities (g/cm^3)		
	Dry sample	Saturated sample	Real density
REF	2.233	2.366	2.575
STN	2.256	2.376	2.563
STS	2.247	2.368	2.555
CA	2.286	2.427	2.660
SF	2.262	2.375	2.550

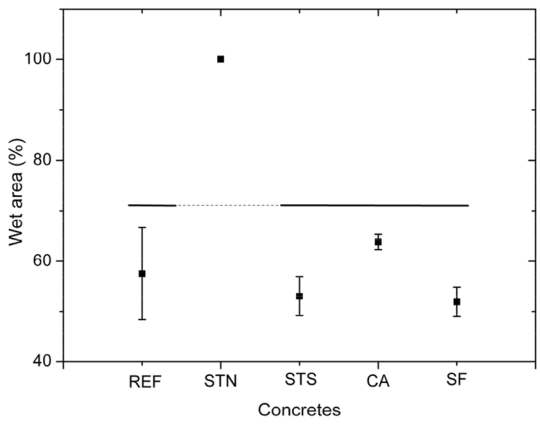

Fig. 3 Wet area average for the studied concretes

4.2 Durability tests

4.2.1 Under pressure water penetration

The results of this test allow analysing concrete permeability through under pressure water penetration. Figure 3 shows the average values of the results for each concrete and the associated standard deviations. It is possible to observe that due to the variability presented by the REF concrete, practically all other concretes, the STS, CA, and SF were considered similar by Fisher's test, represented by the continuous line on the results in the graph. The standard deviation of STN concrete was zero since all samples had a 100% wet area. The concrete STN behaved differently, as it showed a total wetted area, which can also be seen in Fig. 4, which offers an example of the specimens' aspects after splitting. This behaviour was different from expected since coatings/surface treatment must show breathability with adequate water steam permeability [1].

As visible in Figs. 3 and 4, the smoothing process (STS) was beneficial, unlike STN. It can be explained because the

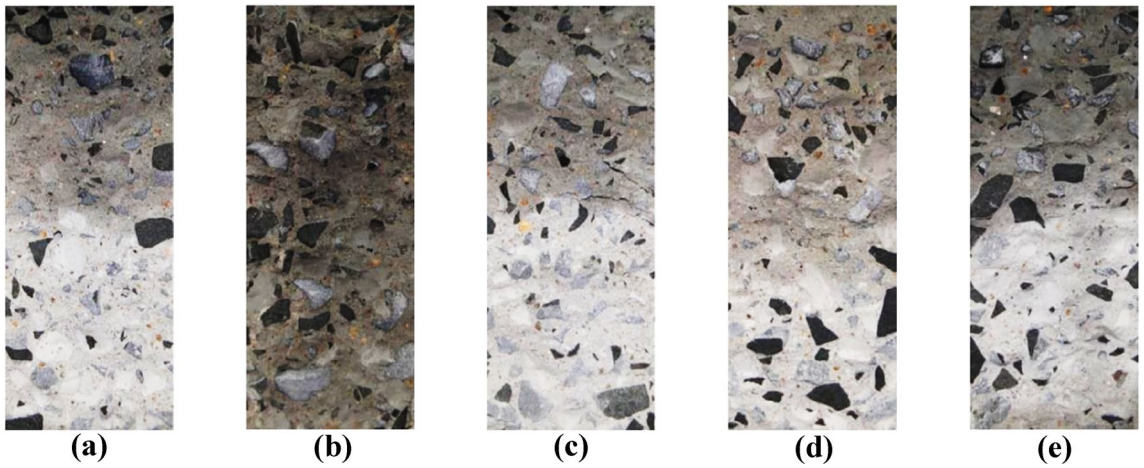

Fig. 4 Specimens aspects after pressure water penetration test **a** REF; **b** STN; **c** STS; **d** CA; **e** SF

non-smoothed surface treatment acted as a physical barrier to the crystalline admixture to penetrate porosity, which allowed for water permeability. However, unlike the other concrete, water steam was not allowed to pass from the concrete to the outside, as the permeated water was trapped inside the sample. The other concrete allowed this evaporation of water throughout the test. Thus, the crystalline admixture product used as a surface treatment without the smoothing process did not perform the function of allowing water steam to pass through, contradicting the characteristics that coatings should have water steam permeability capacity [1].

4.2.2 Carbonation

This test allows for an evaluation of the performance of concrete regarding carbon dioxide permeability. Figure 5a shows the results of carbonation depth in millimetres over the ages of 78, 100, 120, 142, 162, and 176 days. The concrete specimens that received the surface treatment (STN and STS) presented greater carbonation depth, and the REF concrete, the CA and SF concrete presented the lowest carbonation depth. Figure 5b shows the average carbonation depth at 176 days, with their respective standard deviations.

A cross-factor variance analysis was performed for the last test age, 176 days Fig. 5b. It was found that the use of different materials gives statistical significance concerning the REF concrete. There is no significant difference in the results obtained for STN and STS concrete to REF concrete by Fisher's test. However, CA and SF concrete are statistically different from REF concrete but equivalent to each other. Research with a similar CA product also found good performance in terms of resistance to carbonation compared to concretes without adding the product [17].

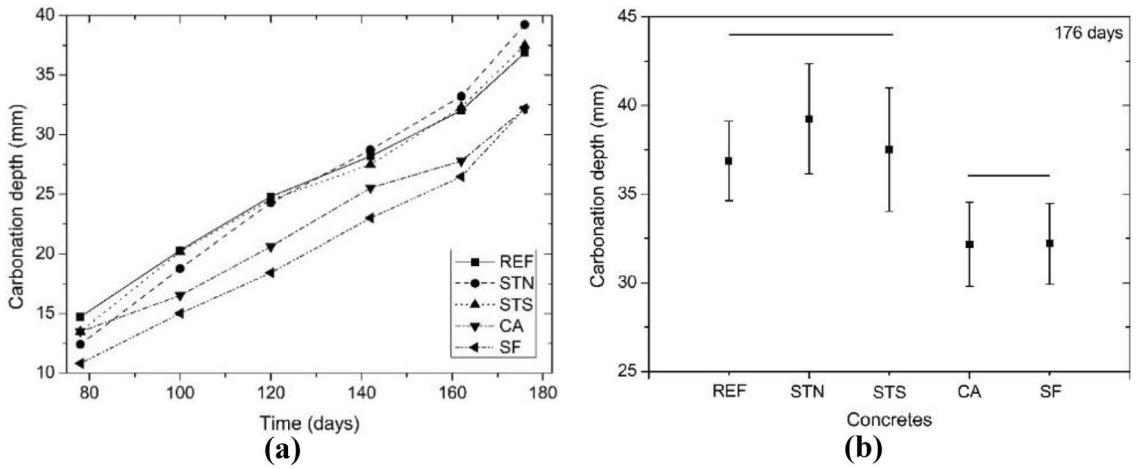

Fig. 5 Carbonation depth **a** over the ages; **b** at 176 days

Among the admixtures used, it was observed, during the phenolphthalein spray, that the SF concrete reduced the pH since the carmine colour due to the chemical spray to higher pH 10.0 had a lower intensity, being pink, i.e., with a pH between 8.3 and 10.0 Fig. 6e. This fact is explained in literature [2] and occurs due to the consumption of calcium hydroxide in the pozzolanic reaction. It can be seen from the image that CA concrete did not have the same influence on pH reduction, as the colour was more intense. Other authors have presented higher pH values for mixtures with CA compared with reference mixtures. This factor tends to favour the precipitation of calcium carbonate [20]. The calcium carbonate precipitation contributes to reducing the capillary porosity and potentiality to the self-healing properties. This fact is essential owing to the understanding of the product, so it is comprehended that high-intensity pozzolanic reactions are not part of the crystalline admixture action system.

STN and STS concrete had no performance improvement. One crucial factor observed was some failures in surface protection regarding the spalling and shrinkage of the protection layer Fig. 7. This can be explained by the fact that the samples are made of dense and robust concrete, which is sufficient to maintain moisture within the pores. As they had a surface treatment layer applied like paint, the internally confined water slowly evaporated during the test due to the lower relative humidity inside the carbonation chamber. The moisture may have caused bubbles, similar to what occurs in ordinary paints when subjected to a negative pressure because of substrate moisture problems. However, since it is a rigid protection system, the applied material was spalled, unlike flexible surface treatments. It was expected that the surface treatment was breathable with adequate water steam permeability. Thus, water steam can leave concrete without producing high pressures at the concrete/coating interface, inducing coating delamination or cracking, as observed previously [1, 82]. The STS concrete did not present this detrimental effect. Still, it also did not perform well as it resembled REF concrete, showing that this type of protection and this material cannot be effective for improving this property.

4.2.3 Chloride penetration

The results related to chloride penetration is shown in Fig. 8a. According to ASTM C 1202 (ASTM 2019) classification, REF concrete and STN, STS, and CA concrete are within the range of penetration of chloride ions ranging from 1000 to 2000 Coulombs, which is considered to be low penetration. SF concrete, however, was in the range of 100–1000 Coulombs, which is relatively meagre. STN and STS concrete showed a slight difference from the REF concrete, STN had a 1% reduction in chloride ion permeability, and STS had a 4% reduction. At the same time, by statistical results, they are equal.

Conversely, CA concrete showed a 29% reduction in permeability to REF concrete, an outcome close to that found by other researchers [9, 33]. SF concrete showed a 75% reduction compared to REF concrete, presenting better performance among the tested concrete. Neville [31] describes

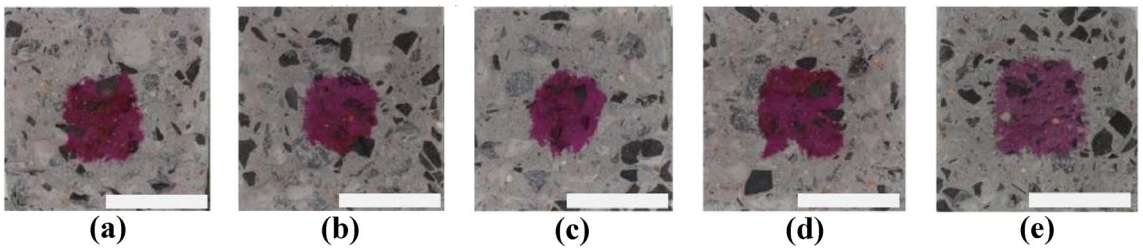

Fig. 6 Aspects of specimens after carbonation test at 176 days, the scale bar below measures 50 mm **a** REF; **b** STN; **c** STS; **d** CA; **e** SF

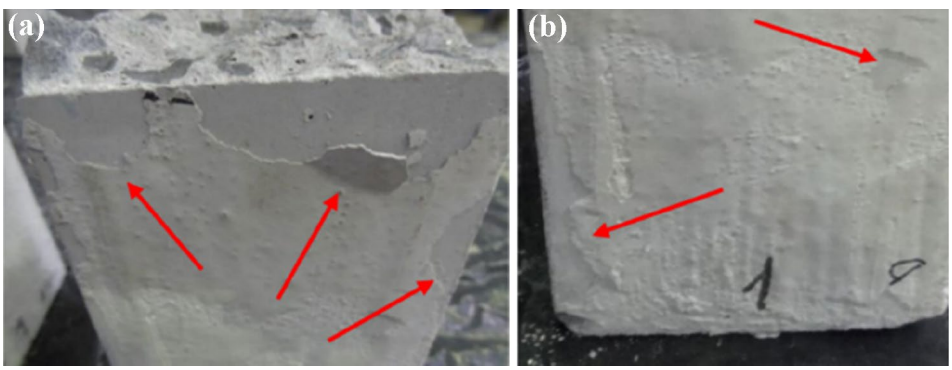

Fig. 7 Aspects of non-smoothing surface treatment (STN) specimens during the carbonation test: details of product drying and peeling **a** some failures in the process of surface protection; **b** spalling and shrinkage of the protection layer

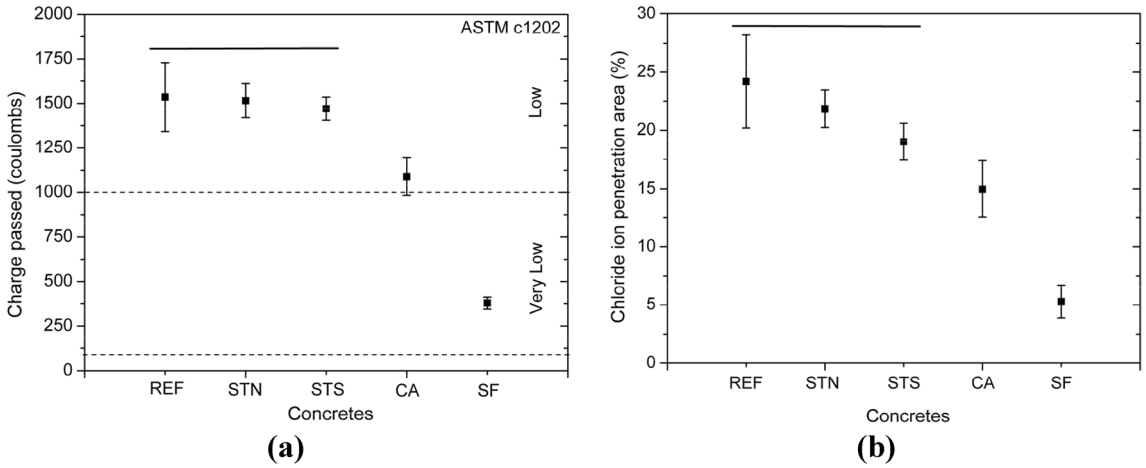

Fig. 8 Chloride penetration **a** charge penetration by ASTM C1202; **b** chloride ion penetration area by silver nitrate spray

this benefit generated by silica fume in the concrete mix due to the increased resistance to chloride ion ingress due to the reduced permeability.

Figure 8(b) shows the results related to chloride penetration with silver nitrate spray. It is possible to observe the exact behaviour according to ASTM C 1202 since the penetration depth of chloride ions is directly related to the total passing charge measured by the test.

Surface treatments should reduce chloride penetration. Other research has shown that coatings act as a physical barrier, reducing water and chloride content into the concrete [1]. In this paper, the surface treatment showed a similar performance to reference concrete.

4.3 Self-healing tests

4.3.1 Ultrasonic pulse propagation

Due to the presence of product formed over time, a self-healing process is expected. Figure 9 shows the evolution of ultrasonic wave propagation velocity for concretes before cracking and after different ages. The measurement taken at 28 days is the velocity in the uncracked specimen and at the age of 51 days after crack creation. It is noted that the velocity is already much lower, which indicates that the damage has already occurred. Then, under the exposure conditions imposed on the samples, the recovery begins in all concretes. The results have shown a great variation, and no mathematically significant differences can be identified between them. In other studies, this fact was observed and reported by Ferrara et al. [94] in the research that analyses methods of self-healing properties. In this specific case, the behaviour is due to how the test is performed because microcracks are created during the rupture in the sample, and these microcracks are randomly

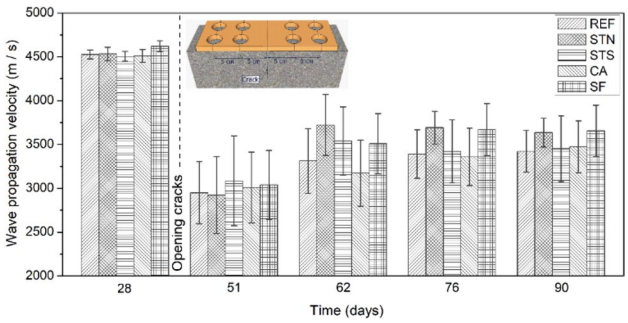

Fig. 9 Wave propagation velocity in different times of exposure

arranged. Therefore, by varying the measuring point along the sample, this velocity depends on the number of cracks it finds in the path. This variation that is not a controllable factor increases the variability of the result, which is in agreement with other papers [92, 93].

However, analysing just the average values, the pulse propagation velocity tends to increase over time. It can be used to indicate the self-healing process, but more analysis is necessary to confirm the phenomenon. One additional factor related to these results can be associated with the initial or not effective self-healing. According to other research, the most effective way to improve the self-healing process is an exposure condition [14] with high water availability [10, 11, 14, 21], as submerged [10, 14, 21, 24, 26]. Hence, in conditions with less availability, there is no evidence of significant changes [10, 11, 26] which may be the case of this study. An exposure environment without water attainability was used, and this condition may have influenced the result and reduced the self-healing products formed. This fact is essential to reassure the need for water once the product does not perform well without high water available.

4.3.2 Scanning electron microscopy (SEM)

SEM analysed the REF, CA and SF concrete, and the images are shown in Fig. 10. Concretes with superficial treatment (STN and STS) were not analysed. The photos obtained correspond to the pieces of concrete removed from regions with cracks. The images correspond to one of the crack walls to allow the observation of products formed under such conditions. All the samples were exposed to a climate chamber for 140 days and then in a humidity chamber for 210 days.

With regards to REF concrete, Fig. 10a, produced using a Brazilian cement with the addition of fly ash, as described previously, it is possible to observe the presence of some spherical grains, characteristic of fly ash in partial dissolution of the surface and regions with the total dissolution of the grain. These images indicate that part of this pozzolan reacts with the high alkalinity generated during the hydration process of the anhydrous phases of cement. The shape of the product formed at the surface of the particles, where there was dissolution and the type of reaction, indicates the formation of hydrated products as secondary C–S–H.

On the other hand, the addition of CA (Fig. 10b) provides the formation of a reaction product with different morphology, in that case in the form of needles. This crystalline structure with needle-shaped crystals is a typical product of self-healing materials. Under the compositions of the admixture used, this case is especially ettringite crystals (mineral of aluminium sulphate and hydrated calcium). Other authors observed similar morphology in researches with similar products [10, 20, 26, 28, 94].

The addition of silica fume (Fig. 10c) increases the amount of pozzolanic materials in the mixture, requiring more time to enable the entire dissolution of the particles. At the same time, the silica fume presents smaller and more reactive particles, which tend to react before the fly ash and form a hydrating product rich in silica. Slight differences in the morphology of the formed products can be observed between Fig. 10a, c, which correspond to the different phases of C–S–H formed.

In these three concretes analysed, the self-healing product formed is different, as well as its mechanism. To allow for the evaluation and differentiation of the

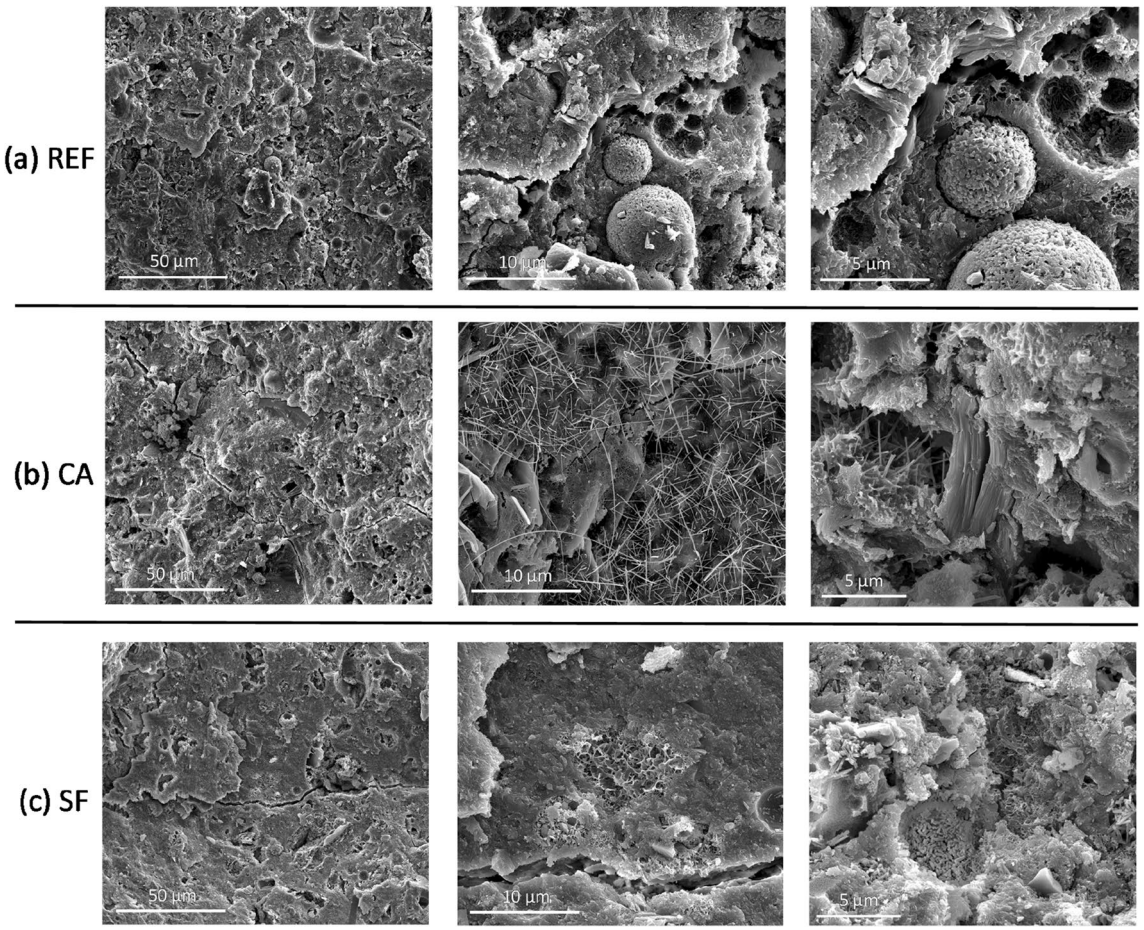

Fig. 10 SEM images of concrete samples in different magnifications **a** REF; **b** CA; **c** SF

developed products, an analysis of elemental energy-dispersive X-ray spectroscopy (EDS) was made by mapping the area of SEM in the SF concrete (Fig. 11). Initially it is possible to observe the presence of different morphologies, such as calcium-silicate-hydrate products, unreactive fly ash from cement and silica fume used as admixture. Figure 11c–e shows different content of Ca, Si and Al, especially in the grains and around them, which makes clear that the total pozzolanic reaction did not occur. One of the leading products of self-healing is calcium carbonate, which can exist in six different forms: calcite, aragonite, vaterite, monohydrocalcite, ikaite and amorphous calcium carbonate [95, 96]. The carbonates create bigger crystals that can fill small cracks easily; however, to make these crystals it is necessary that portlandite is generated during the hydration process of calcium silicate phases. The cement used in this study is pozzolanic cement, so most portlandite was consumed in the pozzolanic reaction, and big crystals of portlandite are not commonly seen. It does not mean that self-healing will not happen for this cement type, but the mechanism will be different, and in that case, the product will be the secondary C–S–H, which has smaller, more stable and more resistant crystals.

5 Conclusion

This study analysed the influence of crystalline admixture used as admixture (CA), as surface treatment (STS and STN), and compared to concrete with silica fume (SF) and without (REF). The highlighted conclusions are:

- The crystalline admixture, used as superficial treatment, is not the most effective solution to provide a more durable material. The water absorption was slightly reduced, however, other properties were not improved. The STN concrete was not breathable without adequate water steam permeability. It can be seen in the under-pressure water penetration test by the complete wet area and the carbonation test by the delamination of the surface treatment;
- The use of CA as admixture did not change the properties of fresh concretes and improved the properties of hardened concretes, providing a reduction in the penetration of chloride and carbonation without compromising the mechanical properties;
- The SF concrete was the solution that presented the best performance, increasing the compressive strength, blocking the entry of chloride, carbonation, reducing water absorption and decreasing the voids index;

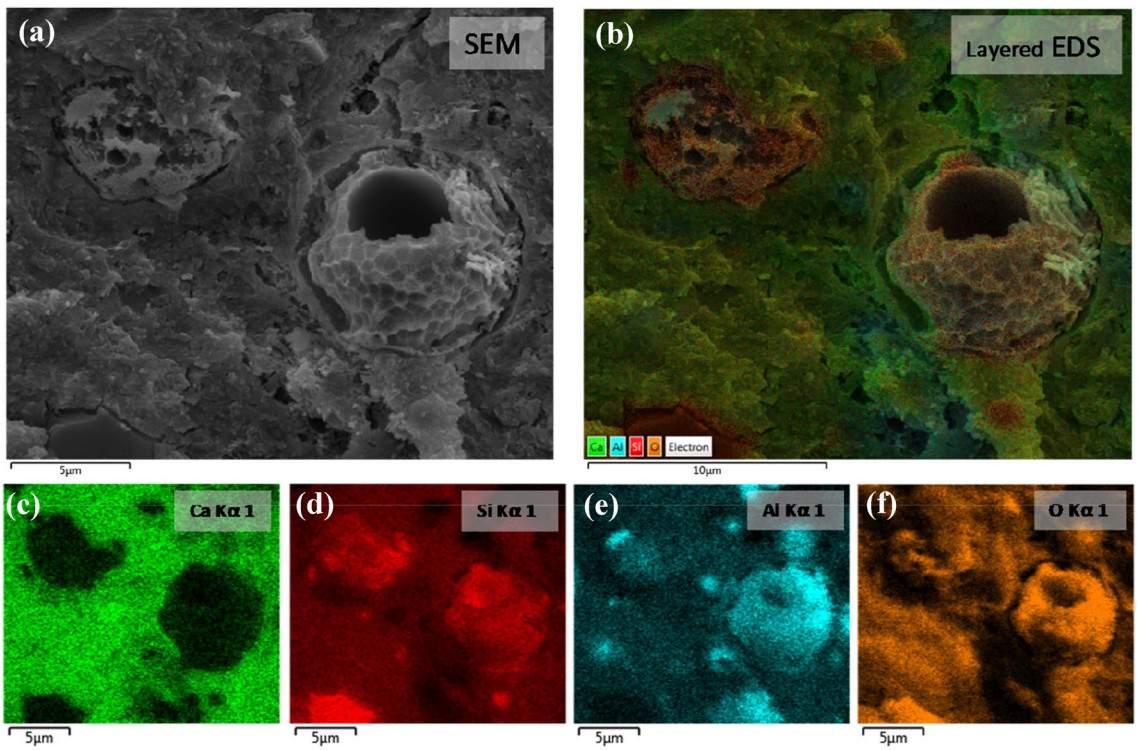

Fig. 11 SEM images and EDS elemental maps of the SF concrete

- The use of an ultrasonic pulse propagation test does not provide an accurate and quantitative value related to self-healing. However, it is an essential factor to indicate the behaviour of product formation over time;
- The self-healing products depend on the materials applied as healing agents. The reference concrete (REF), due to the high amount of fly ash, provides the formation of C-S–H as the main product. The same is observed in silica fume (SF) concrete. By using crystalline admixture, the appearance of different morphology products in the shape of crystals can be attributed to ettringite production.

Acknowledgements The authors would like to thank the LNNano for technical support during electron microscopy work (proposal SEM 24390) and the Laboratório Materiais e Tecnologia do Ambiente Construído (LAMTAC/UFRGS) for technical support during all analysis.

Funding Participation of Brazilian authors was sponsored by CNPq (Brazilian National Council for Scientific and Technological Development) through the research fellowships PQ 310956/2016–1 and PQ 311295/2019–3.

Data availability statement All data, models, and code generated or used during the study appear in the submitted article.

Declarations

Conflict of interest The authors declare that they have no known competing financial interests or personal relationships that could have appeared to influence the work reported in this paper.

References

1. Diamanti MV, Brenna A, Bolzoni F, Berra M, Pastore T, Ormellese M (2013) Effect of polymer modified cementitious coatings on water and chloride permeability in concrete. Constr Build Mater 49:720–728. https://doi.org/10.1016/j.conbuildmat.2013.08.050
2. Mehta PK, Monteiro PJM (2014) Concreto: microestrutura, propriedades e materiais, 2da edição, IBRACON, São Paulo
3. Weisheit S, Unterberger SH, Bader T, Lackner R (2016) Assessment of test methods for characterizing the hydrophobic nature of surface-treated High Performance Concrete. Constr Build Mater 110:145–153. https://doi.org/10.1016/j.conbuildmat.2016.02.010
4. Drochytka R, Ledl M, Bydzovsky J, Zizkova N, Bester J (2019) Use of secondary crystallization and fly ash in waterproofing materials to increase concrete resistance to aggressive gases and liquids. Adv Civ Eng. https://doi.org/10.1155/2019/7530325
5. Coppola L, Coffetti D, Crotti E (2018) Innovative carboxylic acid waterproofing admixture for self-sealing watertight concretes. Constr Build Mater 171:817–824. https://doi.org/10.1016/j.conbuildmat.2018.03.201
6. A. concrete Institute (2010) ACI 212 - Report on chemical admixtures for concrete.
7. Hou P, Cheng X, Qian J, Shah SP (2014) Effects and mechanisms of surface treatment of hardened cement-based materials with colloidal nanoSiO_2 and its precursor. Constr Build Mater 53:66–73. https://doi.org/10.1016/j.conbuildmat.2013.11.062
8. Chandra Sekhara Reddy T, Ravitheja A (2019) Macro mechanical properties of self healing concrete with crystalline admixture under different environments. Ain Shams Eng J 10:23–32. https://doi.org/10.1016/j.asej.2018.01.005
9. Azarsa P, Gupta R, Biparva A (2019) Assessment of self-healing and durability parameters of concretes incorporating crystalline admixtures and Portland Limestone Cement. Cem Concr Compos 99:17–31. https://doi.org/10.1016/j.cemconcomp.2019.02.017
10. Ferrara L, Krelani V, Carsana M (2014) A "fracture testing" based approach to assess crack healing of concrete with and without crystalline admixtures. Constr Build Mater 68:535–551. https://doi.org/10.1016/j.conbuildmat.2014.07.008
11. Roig-Flores M, Moscato S, Serna P, Ferrara L (2015) Self-healing capability of concrete with crystalline admixtures in different environments. Constr Build Mater 86:1–11. https://doi.org/10.1016/j.conbuildmat.2015.03.091
12. Li R, Hou P, Xie N, Ye Z, Cheng X, Shah SP (2018) Design of SiO_2/PMHS hybrid nanocomposite for surface treatment of cement-based materials. Cem Concr Compos 87:89–97. https://doi.org/10.1016/j.cemconcomp.2017.12.008
13. Khanzadeh Moradllo M, Sudbrink B, Ley MT (2016) Determining the effective service life of silane treatments in concrete bridge decks. Constr Build Mater 116:121–127. https://doi.org/10.1016/j.conbuildmat.2016.04.132
14. Borg RP, Cuenca E, Gastaldo Brac EM, Ferrara L (2018) Crack sealing capacity in chloride-rich environments of mortars containing different cement substitutes and crystalline admixtures. J Sustain Cem Mater 7:141–159. https://doi.org/10.1080/21650373.2017.1411297
15. Escoffres P, Desmettre C, Charron JP (2018) Effect of a crystalline admixture on the self-healing capability of high-performance fiber reinforced concretes in service conditions. Constr Build Mater 173:763–774. https://doi.org/10.1016/j.conbuildmat.2018.04.003
16. Huang H, Ye G, Qian C, Schlangen E (2016) Self-healing in cementitious materials: materials, methods and service conditions. Mater Des 92:499–511. https://doi.org/10.1016/j.matdes.2015.12.091
17. Žižková N, Nevřivová L, Lédl M (2018) Durability of cement based mortars containing crystalline additives. Defect Diffus Forum 382:246–253. https://doi.org/10.4028/www.scientific.net/DDF.382.246
18. Sudbrink B, Khanzadeh Moradllo M, Hu Q, Ley MT, Davis JM, Materer N, Apblett A (2017) Imaging the presence of silane coatings in concrete with micro X-ray fluorescence. Cem Concr Res 92:121–127. https://doi.org/10.1016/j.cemconres.2016.11.019
19. Sandrolini F, Franzoni E, Pigino B (2012) Ethyl silicate for surface treatment of concrete—Part I: Pozzolanic effect of ethyl silicate. Cem Concr Compos 34:306–312. https://doi.org/10.1016/j.cemconcomp.2011.12.003
20. Sisomphon K, Copuroglu O (2011) Self healing mortars by using different cementitious materials. In: Proc. Int. Conf. Adv. Constr. Mater. through Sci. Eng. Hong Kong, China, pp. 5–7. http://rilem.net/gene/main.php?base=05&id_publication=407&id_papier=7585.
21. Sisomphon K, Copuroglu O, Koenders EAB (2012) Self-healing of surface cracks in mortars with expansive additive and crystalline additive. Cem Concr Compos 34:566–574. https://doi.org/10.1016/j.cemconcomp.2012.01.005
22. Jiang Z, Li W, Yuan Z, Yang Z (2014) Self-healing of cracks in concrete with various crystalline mineral additives in underground environment. J Wuhan Univ Technol Mater Sci Ed 29:938–944. https://doi.org/10.1007/s11595-014-1024-2
23. Muhammad NZ, Keyvanfar A, Muhd MZ, Shafaghat A, Mirza J (2015) Waterproof performance of concrete: a critical review on

implemented approaches. Constr Build Mater 101:80–90. https://doi.org/10.1016/j.conbuildmat.2015.10.048
24. Roig-Flores M, Pirritano F, Serna P, Ferrara L (2016) Effect of crystalline admixtures on the self-healing capability of early-age concrete studied by means of permeability and crack closing tests. Constr Build Mater 114:447–457. https://doi.org/10.1016/j.conbuildmat.2016.03.196
25. Cappellesso VG, dos Santos Petry N, Dal Molin DCC, Masuero AB (2016) Use of crystalline waterproofing to reduce capillary porosity in concrete. J Build Pathol Rehabil 1:1–12. https://doi.org/10.1007/s41024-016-0012-7
26. Cuenca E, Tejedor A, Ferrara L (2018) A methodology to assess crack-sealing effectiveness of crystalline admixtures under repeated cracking-healing cycles. Constr Build Mater 179:619–632. https://doi.org/10.1016/j.conbuildmat.2018.05.261
27. Roig-Flores M, Litina C, Al-Tabbaa A, Serna P (2018) Capacidad de autosanación de mortero con aditivos cristalinos mediante absorción capilar.https://doi.org/10.4995/hac2018.2018.5831
28. Park B, Choi YC (2018) Self-healing capability of cementitious materials with crystalline admixtures and super absorbent polymers (SAPs). Constr Build Mater 189:1054–1066. https://doi.org/10.1016/j.conbuildmat.2018.09.061
29. Wang L, Zhang G, Wang P, Yu S (2018) Effects of fly ash and crystalline additive on mechanical properties of two-graded roller compacted concrete in a high RCC arch dam. Constr Build Mater 182:682–690. https://doi.org/10.1016/j.conbuildmat.2018.06.101
30. Al-harahsheh MS, Al K, Al-makhadmeh L, Hararah M, Mahasneh M (2015) Fly ash based geopolymer for heavy metal removal: a case study on copper removal. J Environ Chem Eng 3:1669–1677
31. Neville A (2016) Propriedades do concreto, 5th ed., Bookman, Porto Alegre.
32. Murakami T, Ahn TH, Hashimoto T, Ogura N, Kishi T, Shim KB (2015) A study on new repair methods for subway tunnels using crack self-healing technologies. J Ceram Process Res 16:s95–s97
33. Helene P, Guignone G, Vieira G, Roncetti L, Moroni F (2018) Avaliação da penetração de cloretos e da vida útil de concretos autocicatrizantes ativados por aditivo cristalino. RIEM IBRACON Struct Mater J 11.
34. Şahmaran M, Keskin SB, Ozerkan G, Yaman IO (2008) Self-healing of mechanically-loaded self consolidating concretes with high volumes of fly ash. Cem Concr Compos 30:872–879. https://doi.org/10.1016/j.cemconcomp.2008.07.001
35. Ahn TH, Kishi T (2010) Crack self-healing behavior of cementitious composites incorporating various mineral admixtures. J Adv Concr Technol 8:171–186. https://doi.org/10.3151/jact.8.171
36. Huang H, Ye G (2011) Application of sodium silicate solution as self-healing agent in cementitious materials Outline • Introduction • Materials and experiments • Results and discussion Problems Research objective, pp 1–9.
37. Huang H, Ye G, Damidot D (2014) Effect of blast furnace slag on self-healing of microcracks in cementitious materials. Cem Concr Res 60:68–82. https://doi.org/10.1016/j.cemconres.2014.03.010
38. Ma H, Qian S, Zhang Z (2014) Effect of self-healing on water permeability and mechanical property of Medium-Early-Strength Engineered Cementitious Composites. Constr Build Mater 68:92–101. https://doi.org/10.1016/j.conbuildmat.2014.05.065
39. Maes M, Snoeck D, De Belie N (2016) Chloride penetration in cracked mortar and the influence of autogenous crack healing. Constr Build Mater 115:114–124. https://doi.org/10.1016/j.conbuildmat.2016.03.180
40. Suleiman AR, Nehdi ML (2018) Effect of environmental exposure on autogenous self-healing of cracked cement-based materials. Cem Concr Res 111:197–208. https://doi.org/10.1016/j.cemconres.2018.05.009
41. Wang X, Fang C, Li D, Han N, Xing F (2018) A self-healing cementitious composite with mineral admixtures and built-in carbonate. Cem Concr Compos 92:216–229. https://doi.org/10.1016/j.cemconcomp.2018.05.013
42. Pedro D, de Brito J, Evangelista L (2018) Durability performance of high-performance concrete made with recycled aggregates, fly ash and densified silica fume. Cem Concr Compos 93:63–74. https://doi.org/10.1016/j.cemconcomp.2018.07.002
43. Lewis RC (2018) Silica Fume BT—properties of fresh and hardened concrete containing supplementary cementitious materials: state-of-the-art report of the rilem technical committee 238-SCM, Working Group 4. https://doi.org/10.1007/978-3-319-70606-1_3.
44. Bissonnete B, Pigeon M (1995) Tensile creep at early ages of ordinary, silica fume and fiber reinforced concretes. Cem Concr Res 25:1075–1085
45. Bhanja S, Sengupta B (2005) Influence of silica fume on the tensile strength of concrete. Cem Concr Res 35:743–747. https://doi.org/10.1016/j.cemconres.2004.05.024
46. Rashad AM (2015) A brief on high-volume class F fly ash as cement replacement—a guide for civil engineer. Int J Sustain Built Environ Cl. https://doi.org/10.1016/j.ijsbe.2015.10.002
47. Enfedaque Díaz A, Sánchez Paradela L, Sánchez-Gálvez V (2010) El efecto del humo de sílice y el metacaolín en el proceso de envejecimiento de los morteros de cemento reforzados con fibras de vidrio (GRC). Mate. Constr 60:67–82. https://doi.org/10.3989/mc.2010.52009
48. Inan Sezer G (2012) Compressive strength and sulfate resistance of limestone and/or silica fume mortars. Constr Build Mater 26:613–618. https://doi.org/10.1016/j.conbuildmat.2011.06.064
49. Van den Heede P, Maes M, De Belie N (2014) Influence of active crack width control on the chloride penetration resistance and global warming potential of slabs made with fly ash+silica fume concrete. Constr Build Mater 67:74–80. https://doi.org/10.1016/j.conbuildmat.2013.10.032
50. Haruehansapong S, Pulngern T, Chucheepsakul S (2014) Effect of the particle size of nanosilica on the compressive strength and the optimum replacement content of cement mortar containing nano-SiO_2. Constr Build Mater 50:471–477. https://doi.org/10.1016/j.conbuildmat.2013.10.002
51. Biricik H, Sarier N (2014) Comparative study of the characteristics of nano silica-, silica fume- and fly ash-incorporated cement mortars. Mater Res 17:570–582. https://doi.org/10.1590/S1516-14392014005000054
52. Çakır Ö, Sofyanlı ÖÖ (2015) Influence of silica fume on mechanical and physical properties of recycled aggregate concrete. HBRC J 11:157–166. https://doi.org/10.1016/j.hbrcj.2014.06.002
53. Bhalla N, Sharma S, Sharma S, Siddique R (2018) Monitoring early-age setting of silica fume concrete using wave propagation techniques. Constr Build Mater 162:802–815. https://doi.org/10.1016/j.conbuildmat.2017.12.032
54. American Society for Testing and Materials (2013) ASTM C595/595M-13: Standard Specification for Blended Hydraulic Cements
55. ANBT (2019) NBR 16697: Portland cement - Requirements
56. Associaçao_Brasileira_de_Normas_Técnicas (2018) NBR 16607: Portland cement—Determination of setting times
57. A.B. de N.T. ABNT (2019) NBR 7215—Portland cement—Determination of compressive strength of cylindrical test specimens
58. Guo Z, Jiang T, Zhang J, Kong X, Chen C, Lehman DE (2020) Mechanical and durability properties of sustainable self-compacting concrete with recycled concrete aggregate and fly ash, slag and silica fume. Constr Build Mater 231:117115. https://doi.org/10.1016/j.conbuildmat.2019.117115
59. Falmata AM, Sulaiman A, Mohamed RN, Shettima AU (2020) Mechanical properties of self-compacting high-performance concrete with fly ash and silica fume. SN Appl Sci 2:1–11. https://doi.org/10.1007/s42452-019-1746-z

60. Wang D, Zhang Y, Hong Z (2014) Novel fast-setting chitosan/β-dicalcium silicate bone cements with high compressive strength and bioactivity 40:9799–9808
61. Jozwiak-Niedzwiedzka D (2015) Microscopic observations of self-healing products in calcareous fly ash mortars. Microsc Res Tech 78:22–29. https://doi.org/10.1002/jemt.22440
62. Associaçao_Brasileira_de_Normas_Técnicas (2003) NBR NM 248: Aggregates—Sieve analysis of fine and coarse aggregates
63. Associaçao_Brasileira_de_Normas_Técnicas (2009) NBR NM 52 Fine aggregate—Determination of the bulk specific gravity and apparent specific gravity
64. Associaçao_Brasileira_de_Normas_Técnicas (2017) NBR 16605: Portland cement and other powdered material—Determination of the specific gravity
65. American Society for Testing and Materials (2017) ASTM C494/C494M: standard specification for chemical admixtures for concrete
66. Liu Z, Hansen W (2016) Effect of hydrophobic surface treatment on freeze-thaw durability of concrete. Cem Concr Compos 69:49–60. https://doi.org/10.1016/j.cemconcomp.2016.03.001
67. Nishiwaki T, Sasaki H, Kwon SM (2015) Experimental study on self-healing effect of FRCC with PVA fibers and additives. J Ceram Process Res 16:89s–94s
68. Associaçao_Brasileira_de_Normas_Técnicas, NBR NM 67 (1998) Concrete—Slump test for determination of the consistency
69. Associaçao_Brasileira_de_Normas_Técnicas, BNR 5739 - Concrete - Compression test of cylindrical specimes, 2018.
70. Associaçao_Brasileira_de_Normas_Técnicas (2005) NBR 9778—Hardened mortar and concrete - Determination of absorption, voids and specific gravity..
71. American Society for Testing & Materials C 1202 (2019) Standard Test Method for Electrical Indication of Concrete's Ability to Resist Chloride Ion Penetration
72. American Society for Testing and Materials (2016) ASTM C597: standard test method for pulse velocity through concrete.
73. Van Tittelboom K, De Belie N, De Muynck W, Verstraete W (2010) Use of bacteria to repair cracks in concrete. Cem Concr Res 40:157–166. https://doi.org/10.1016/j.cemconres.2009.08.025
74. Xu J, Yao W (2014) Multiscale mechanical quantification of self-healing concrete incorporating non-ureolytic bacteria-based healing agent. Cem Concr Res 64:1–10. https://doi.org/10.1016/j.cemconres.2014.06.003
75. Mostavi E, Asadi S, Hassan MM, Alansari M (2015) Evaluation of self-healing mechanisms in concrete with double-walled sodium silicate microcapsules. J Mater Civ Eng 27:04015035. https://doi.org/10.1061/(ASCE)MT.1943-5533.0001314
76. Krelani V, Krelani V, Moretti F (2016) Autogenous healing on the recovery of mechanical performance of high performance fibre reinforced cementitious composites (HPFRCCs): Part 2—correlation between healing of mechanical performance and crack sealing. Cem Concr Compos 73:299–315. https://doi.org/10.1016/j.cemconcomp.2016.08.003
77. Williams RP, van Riessen A (2016) The first 20 hours of geopolymerization: an in situ WAXS study of flyash-based geopolymers. Mater (Basel) 9:1–13. https://doi.org/10.3390/MA9070552
78. Ferrara L, Krelani V, Moretti F (2016) On the use of crystalline admixtures in cement based construction materials : from porosity reducers to promoters of self healing. Smart Mater Struct 25:17. https://doi.org/10.1088/0964-1726/25/8/084002
79. Ferrara L, Krelani V, Moretti F, Roig Flores M, Serna Ros P (2017) Effects of autogenous healing on the recovery of mechanical performance of High Performance Fibre Reinforced Cementitious Composites (HPFRCCs): Part 1. Cem Concr Compos 83:76–100. https://doi.org/10.1016/j.cemconcomp.2017.07.010
80. Yang K, Song J, Ashour A, . Lee E (2008) Properties of cementless mortars activated by sodium silicate. Constr Build Mater 22:1981–1989. https://doi.org/10.1016/j.conbuildmat.2007.07.003
81. Sherir MAA, Hossain KMA, Lachemi M (2016) Self-healing and expansion characteristics of cementitious composites with high volume fly ash and MgO-type expansive agent. Constr Build Mater 127:80–92. https://doi.org/10.1016/j.conbuildmat.2016.09.125
82. Al-Kheetan MJ, Rahman MM, Chamberlain DA (2017) Influence of early water exposure on modified cementitious coating. Constr Build Mater 141:64–71. https://doi.org/10.1016/j.conbuildmat.2017.02.159
83. Byoungsun P, Young CC (2019) Investigating a new method to assess the self-healing performance of hardened cement pastes containing supplementary cementitious materials and crystalline admixtures. J Mater Res Technol 8:6058–6073. https://doi.org/10.1016/j.jmrt.2019.09.080
84. Li H, Xiao HG, Yuan J, Ou J (2004) Microstructure of cement mortar with nano-particles. Compos Part B Eng 35:185–189. https://doi.org/10.1016/S1359-8368(03)00052-0
85. Wongkeo W, Thongsanitgarn P, Chindaprasirt P, Chaipanich A (2013) Thermogravimetry of ternary cement blends. J Therm Anal Calorim 113:1079–1090. https://doi.org/10.1007/s10973-013-3017-3
86. Yamato K, Sasaki A, Ito T, Yoshitake I (2020) Resistance properties to chloride ingress of standard-cured concrete made with an admixture incorporating rich SiO_2 and Al_2O_3. Int J Concr Struct Mater. https://doi.org/10.1186/s40069-020-0391-7
87. Mazloom M, Ramezanianpour AA, Brooks JJ (2004) Effect of silica fume on mechanical properties of high-strength concrete. Cem Concr Compos 26:347–357. https://doi.org/10.1016/S0958-9465(03)00017-9
88. Peng MX, Wang ZH, Shen SH, Xiao QG, Li LJ, Tang YC, Hu LL (2017) Alkali fusion of bentonite to synthesize one-part geopolymeric cements cured at elevated temperature by comparison with two-part ones. Constr Build Mater. https://doi.org/10.1016/j.conbuildmat.2016.11.010
89. Zhang P, Wittmann FH, Villmann B, Zhao T-J, Slowik V (2008) Moisture diffusion in and capillary suction of integral water repellent cement based materials, Hydrophobe V, pp 273–286.
90. Bertolini L (2010) Materiais de construção: Patologia, reabilitação e prevenção, oficina de, São Paulo.
91. Reiterman P, Pazderka J (2016) Crystalline coating and its influence on the water transport in concrete. Adv Civ Eng. https://doi.org/10.1155/2016/2513514
92. Akhavan A, Shafaatian SMH, Rajabipour F (2012) Quantifying the effects of crack width, tortuosity, and roughness on water permeability of cracked mortars. Cem Concr Res 42:313–320. https://doi.org/10.1016/j.cemconres.2011.10.002
93. Van Mullem T, Gruyaert E, Debbaut B, Caspeele R, De Belie N (2019) Novel active crack width control technique to reduce the variation on water permeability results for self-healing concrete. Constr Build Mater 203:541–551. https://doi.org/10.1016/j.conbuildmat.2019.01.105
94. Gagné R, Argouges M (2012) A study of the natural self-healing of mortars using air-flow measurements. Mater Struct Constr 45:1625–1638. https://doi.org/10.1617/s11527-012-9861-y
95. Krelani V (2015) Self healing capacity of cementitious composites, politecocnico di Milano, pp 102–118.
96. Teghidet H (2013) Etude de la cristallisation contrôlée de la calcite par voie électrochimique . Effet des ions étrangers au système calcocarbonique sur la nucléation-croissance de la calcite. To cite this version : HAL Id : tel-00788536 Spécialité : Electrochimie Sujet